

Improving Visualization of In-stent Lumen Using Prototype Photon-counting Detector Computed Tomography with High-resolution Plaque Kernel

Yoshinori Funama, Seitaro Oda¹, Fuyuhiko Teramoto², Yuko Aoki², Isao Takahashi³, Shinichi Kojima³, Taiga Goto², Kana Tanaka², Masafumi Kidoh¹, Yasunori Nagayama¹, Takeshi Nakaura¹, Toshinori Hirai¹

Departments of Medical Radiation Sciences and ¹Diagnostic Radiology, Faculty of Life Sciences, Kumamoto University, Kumamoto, ²Medical System Research and Development Center, FUJIFILM Healthcare Corporation, ³Innovative Technology Laboratory, FUJIFILM Healthcare Corporation, Tokyo, Japan

Abstract

The study aimed to compare the performance of photon-counting detector computed tomography (PCD CT) with high-resolution (HR)-plaque kernel with that of the energy-integrating detector CT (EID CT) in terms of the visualization of the lumen size and the in-stent stenotic portion at different coronary vessel angles. The lumen sizes in PCD CT and EID CT images were 2.13 and 1.80 mm at 0°, 2.20 and 1.77 mm at 45°, and 2.27 mm and 1.67 mm at 90°, respectively. The lumen sizes in PCD CT with HR-plaque kernel were wider than those in EID CT. The mean degree of the in-stent stenotic portion at 50% was 69.7% for PCD CT and 90.4% for EID CT. PCD CT images with HR-plaque kernel enable improved visualization of lumen size and accurate measurements of the in-stent stenotic portion compared to conventional EID CT images regardless of the stent direction.

Keywords: Energy-integrating detector computed tomography, in-stent plaque visibility, lumen size, photon-counting detector computed tomography

Received on: 28-11-2023

Review completed on: 11-01-2024

Accepted on: 12-01-2024

Published on: 30-03-2024

INTRODUCTION

Coronary computed tomography angiography (CTA) is widely used for the diagnosis of coronary artery disease.^[1-4] Coronary CTA is a potentially useful noninvasive technique for the evaluation of in-stent restenosis.^[5-8] However, in-stent evaluation is challenging because of the small structure of the coronary arterial stent. Moreover, metallic artifacts, partial volume effect, blooming, photon starvation, and beam-hardening effects also affect the visualization.^[9,10] These factors impede visualization of the true in-stent restenosis. According to a study, approximately 12% of all coronary stents cannot be imaged with a diagnostic quality.^[11] The spatial resolution of conventional-resolution computed tomography (CT) may be insufficient for in-stent assessment and high-resolution (HR) imaging is required for determining the plaque composition and structure.^[12]

Combining prototype photon-counting detector CT (PCD CT) with a dedicated HR plaque kernel (FUJIFILM Healthcare

Corporation) is a recently developed technique. In general, PCD CT offers several advantages over the currently used conventional energy-integrating detector CT (EID CT).^[13-16] The prototype PCD CT can be used in the ultra-HR (UHR) mode and multienergy discrimination (MED) mode depending on clinical purposes.^[17] The detector pixel pitch at the isocenter in the MED mode and UHR mode is 0.58 mm × 0.63 mm and 0.19 mm × 0.21 mm, respectively. The UHR mode has been shown to be particularly useful in coronary CTA.^[17] Besides, the HR-plaque kernel is the dedicated kernel for improving image quality in the in-stent lumen. Therefore, compared to conventional EID CT, PCD CT with HR-plaque kernel may further improve the visualization and assessment of coronary

Address for correspondence: Prof. Yoshinori Funama, Department of Medical Radiation Sciences, Faculty of Life Sciences, Kumamoto University, 4-24-1 Kuhonji, Kumamoto 862-0976, Japan. E-mail: funama@kumamoto-u.ac.jp

This is an open access journal, and articles are distributed under the terms of the Creative Commons Attribution-NonCommercial-ShareAlike 4.0 License, which allows others to remix, tweak, and build upon the work non-commercially, as long as appropriate credit is given and the new creations are licensed under the identical terms.

For reprints contact: WKHLRPMedknow_reprints@wolterskluwer.com

How to cite this article: Funama Y, Oda S, Teramoto F, Aoki Y, Takahashi I, Kojima S, *et al.* Improving visualization of in-stent lumen using prototype photon-counting detector computed tomography with high-resolution plaque kernel. *J Med Phys* 2024;49:127-32.

Access this article online

Quick Response Code:



Website:
www.jmp.org.in

DOI:
10.4103/jmp.jmp_163_23

plaques in different coronary vessels in clinical practice. However, the PCD CT images with HR-plaque kernel have not been evaluated in terms of visualization of the lumen size and the in-stent stenotic portion. Therefore, the advantages of PCD CT over EID CT are not clear.

The present study aimed to compare the performance of the prototype PCD CT with HR-plaque kernel as compared to the clinically used conventional EID CT in terms of lumen size and visualization of the in-stent stenotic portion at different coronary vessel angles.

MATERIALS AND METHODS

Coronary vessel model

A vessel tube with a noncalcified plaque in a stent (Fuyo Corporation, Tokyo, Japan) was used as the coronary vessel model [Figure 1]. The length and the lumen diameter of the coronary vessel model were 50.0 and 3.0 mm, respectively. A drug-eluting coronary arterial stent (diameter: 3 mm; strut thickness: 81 μm) (Xience V, Abbott Vascular, Santa Clara, CA, USA) was inserted in the vessel model. The degrees of stepped stenotic plaques inside the lumen were 25%, 50%, and 75%. The material for the simulated plaque was composed of polystyrene designed for a CT number of 80 HU at 120 kVp. The plaque part simulated a noncalcified plaque. In this study, from the clinical perspective, a 50% stenotic portion was measured.^[18] The vessel tube was filled with diluted iodinated contrast medium (Ioberin-300; Takeda-teva.com, Aichi, Japan) to reach a target lumen CT number of approximately 400 HU. The coronary vessel model was fixed at the center of a water-filled polypropylene cylindrical container [diameter: 17.5 cm; height: 11.5 cm; Figure 1].

Computed tomography imaging and image reconstruction

A vessel tube with noncalcified plaque in a 3.0-mm stent was scanned using the prototype PCD CT (FUJIFILM

Healthcare Corporation, Tokyo, Japan) and the conventional EID CT (FUJIFILM Healthcare Corporation, Tokyo, Japan). The conventional axial scan mode was used for both PCD CT and EID CT scans. The coronary vessel model was placed at 15.0 mm off-center position along the x direction with three different angles, i.e., 0°, 45°, and 90°, along the z direction.

The scanner parameters for one PCD CT scan were as follows: tube voltage, 120 kVp; tube current-time product, 300 mAs; detector configuration, 18 mm \times 0.208 mm; slice thickness, 0.208 mm; slice interval, 0.206 mm; display field of view, 35 mm \times 35 mm; and matrix size, 512 \times 512. The scanning parameters for EID CT were detector configuration, 8 mm \times 0.625 mm; slice thickness and interval, 0.625 mm. The other scan parameters were the same as those for PCD CT.

All images were reconstructed using the filtered back projection (FBP) algorithm. HR-plaque reconstruction kernel was applied for FBP image reconstruction with UHR mode on PCD CT. A cardiac stent reconstruction kernel was used for the FBP reconstruction on EID CT.

Lumen size and in-stent stenotic-portion visibility

To analyze the lumen size and the visibility of the in-stent stenotic portion, multiplanar reformations (MPRs) were conducted using the same 0.5-mm slice thickness and 0.2-mm slice interval in PCD CT and EID CT images. The straight line was set at 0.07 mm \times 4.7 mm (1 \times 69 pixels with PCD CT and EID CT images) across both sides of the stent struts with a 50% stenotic portion [Figure 2]. Subsequently, the CT numbers of pixels, including the stent strut, the plaque at 50% stenosis, and the contrast medium portions, were measured, and a profile curve was obtained. The profile curves were obtained from PCD and EID CT images. The lumen size was calculated from the distance

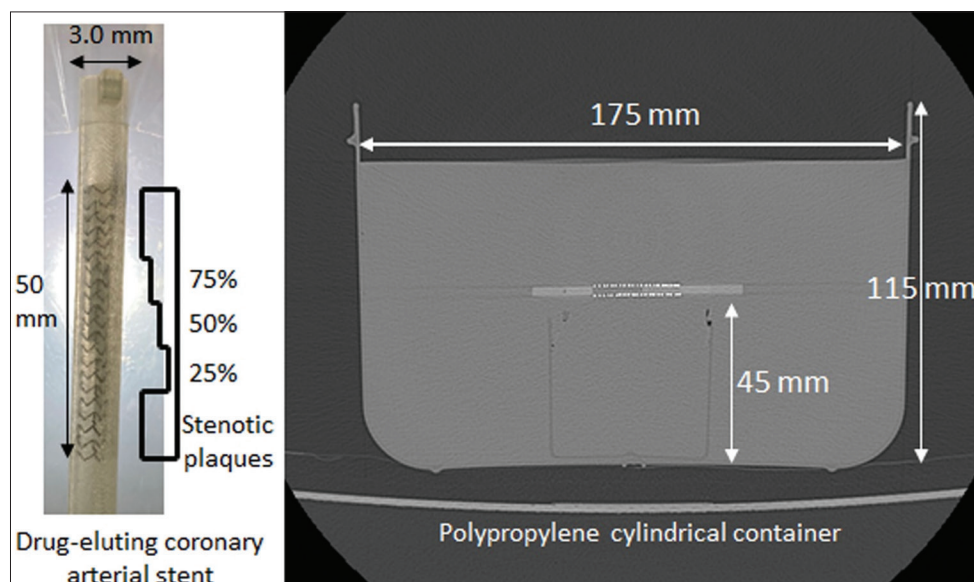


Figure 1: Photograph and schematic of the experiment

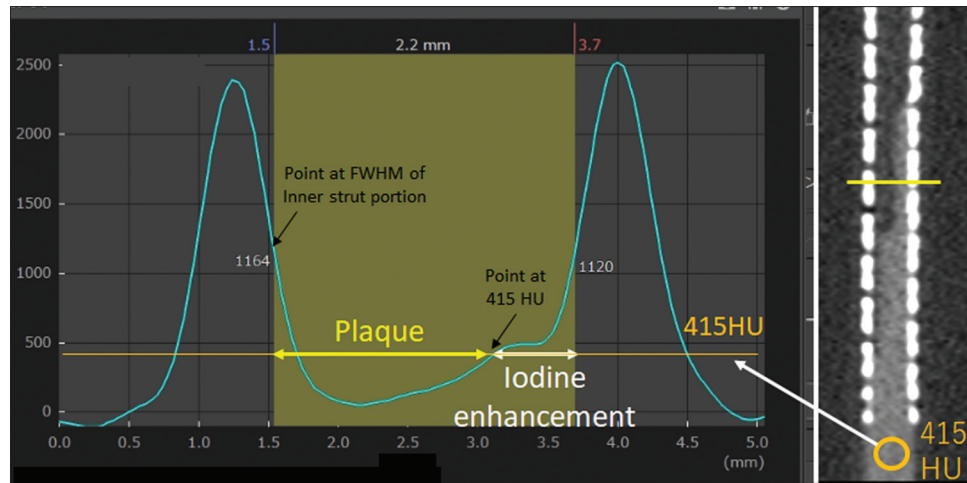


Figure 2: Profile curve at the 0° direction for obtaining photon-counting detector CT. A rectangular region of interest was set across both sides of the stent struts with a 50% stenotic portion on the multiplanar reformation image and the profile curve was obtained. FWHM: Full width at half maximum

between the full width at half maximum (FWHM) values at both sides of the inner strut position. Regarding the in-stent measurements, the cutoff value at the plaque portion and iodine portions was set at 415 HU based on the iodine CT number of the outside portion of the stent [Figure 2]. The extent of the plaque was calculated as the length from the point at FWHM of the inner strut portion on the plaque side to the point at 415 HU of the profile curve [Figure 2]. Finally, the degree of the in-stent stenotic portion was obtained using the following equation,

Degree of in-stent stenotic portion (%) = Length at plaque portion/3.0-mm × 100.

RESULTS

Lumen size

The lumen sizes for PCD CT with HR-plaque kernel and EID CT at stent directions of 0°, 45°, and 90° are shown in Figure 3. The lumen sizes for PCD CT and EID CT images were 2.13 and 1.80 mm at 0°, 2.20 and 1.77 mm at 45°, and 2.27 mm and 1.67 mm at 90°, respectively. The mean lumen size was 2.20 mm for PCD CT and 1.74 mm for EID CT. The lumen sizes assessed by PCD CT with HR-plaque kernel were wider than those assessed by EID CT regardless of the stent direction.

Degree of the in-stent stenotic portion

Figure 4 shows the degree of in-stent stenotic portion visibility with PCD CT with HR-plaque and EID CT. The measurements of the in-stent stenotic portion using PCD CT and EID CT images were 68.8% and 90.7% at 0°, 72.7% and 90.0% at 45°, and 67.6% and 90.0% at 90°, respectively. The mean degree of the in-stent stenotic portion was 69.7% for PCD CT and 90.4% for EID CT. The PCD CT images enabled more accurate measurements of the 50% stenotic portion than EID CT.

Transverse and multiplanar reformation stent images

Figures 5 and 6 show the transverse and MPR stent images at 0°, 45°, and 90° on PCD CT with HR-plaque kernel and EID

CT. The PCD CT images and MPR images with HR-plaque kernel showed better visualization of the stenotic portion and iodine enhancement portions compared to EID CT. Moreover, the PCD CT images and MPR images showed fewer blooming artifacts and better plaque conspicuity and iodine enhancement than EID CT images.

DISCUSSION

The study evaluated the ability of PCD CT with HR-plaque kernel in terms of lumen size and in-stent plaque visibility at different coronary vessel angles of 0°, 45°, and 90° along the z direction compared to conventional EID CT. The PCD CT images showed superior in-stent lumen visibility of the plaque and iodine-enhanced portions than the EID CT images. Besides, PCD CT with HR-plaque kernel achieved wider lumen size and more accurate measurements of the in-stent stenotic portion compared to EID CT regardless of coronary vessel angles.

PCD CT with HR-plaque kernel reduced blooming artifacts and partial volume artifacts and improved the spatial resolution compared to EID CT. In general, the relevant image artifacts on coronary CTA result from poor image quality.^[9] Mannil *et al.*^[10] directly compared PCD CT with the best detection technology currently available in the clinical setting. They observed the best results for PCD technology at 0°- phantom position with markedly improved image quality, 16% better in-stent lumen visualization, and less blooming and partial volume artifacts, reflected in a 37% lower increase in the attenuation of in-stent lumen. Mahnken *et al.*^[9] evaluated the ability to visualize coronary artery lumen in the presence of coronary artery stents. They found that the convolution kernel had the most significant influence on the visibility of the lumen of the individual stents. The modulation transfer function was optimized in this kernel to reduce the blurring that typically occurs close to borders with high attenuation differences. This effect

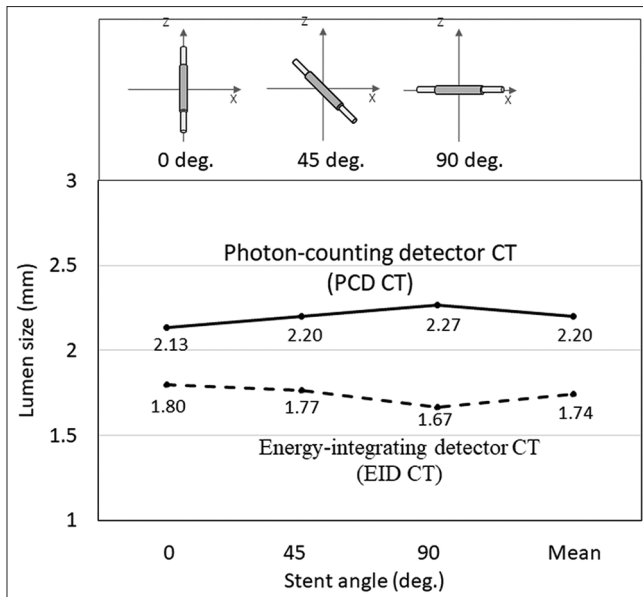


Figure 3: Lumen size assessment with photon-counting detector computed tomography (PCD CT) and energy-integrating detector CT (EID CT). The lumen sizes obtained with PCD CT with high-resolution-plaque kernel were wider than those obtained with EID CT regardless of the stent direction. CT: Computed tomography, PCD: Photon-counting detector, EID: Energy-integrating detector

resulted in a sharper delineation of each stent. Therefore, the dedicated convolution kernel was found to be an essential factor for improving in-stent lumen visualization. They concluded that a combination of PCD CT and HR-plaque reconstruction kernel enables high-quality visualization of the in-stent lumen.

Improved spatial resolution in in-plane and through-plane helps improve the assessment of the stenotic portion of the in-stent lumen. The coronary arteries typically have an oblique course and are often assessed using MPR of the transverse images (axial images). Therefore, in the present study, the stent angle was added at 45° and 90° along the z-axis. The results for the degree of the in-stent stenotic portion on PCD CT were 72.7% and 67.6% for 45° and 90° compared to 90.0% and 90.0% for 45° and 90° on conventional EID CT and more accurate measurements were obtained than conventional EID CT. When using conventional EID CT, Ghekiere *et al.*^[19] suggested that the in-plane spatial resolution is limited to approximately 0.5 mm by the use of smoothing convolution reconstruction algorithms. Although the spatial resolution is sufficient for the assessment of significant coronary artery stenosis in vessels with a diameter of ≥ 1.5 mm, it may be inadequate for assessing the stent patency and to confidently grade coronary stenosis in severely calcified arteries.^[19-21] Unlike EID CT, the detector size and slice thickness used for PCD CT in the study were narrower at 0.208 mm and 0.208 mm, respectively. The in-plane and through-plane resolution are critical factors for improving in-stent plaque visualization.

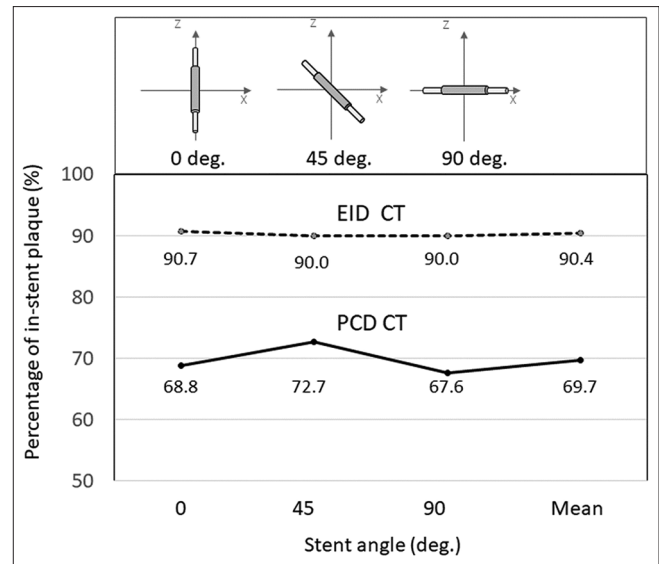


Figure 4: Assessment of the degree of stenosis of the in-stent lumen using photon-counting detector computed tomography (PCD CT) with high-resolution-plaque kernel and energy-integrating detector CT (EID CT). The PCD CT images enabled more accurate measurements of the 50% stenotic portion than EID CT images. CT: Computed tomography, PCD: Photon-counting detector, EID: Energy-integrating detector

Some limitations of this study should be acknowledged. First, the coronary vessel model did not reproduce the motion artifacts derived from the heartbeat. Kojima *et al.*^[22] reported the effect of the heart rate on motion artifact in U-HRCT. They found that U-HRCT is more sensitive to motion than EID CT is. At heart rates ≤ 60 bpm, U-HRCT was more accurate for imaging the coronary arteries than EID CT was. However, the inverse was shown at heart rates > 60 bpm, because the U-HRCT images were strongly affected by motion artifacts. In clinical settings, the image quality of PCD CT tends to be hampered by cardiac motion, irregular pulse, and respiratory movements. To further our findings, future research should consider the effect of the said degraded factors on image quality. Second, as iterative reconstruction (IR) and deep learning reconstruction (DLR) are currently not available for use, we applied one image reconstruction algorithm of FBP. As IR and DLR are useful tools for reducing radiation dose and image noise, further development of the reconstruction algorithms is needed. Finally, the image reconstruction kernel was not applied using the same settings during image reconstructions with PCD CT and EID CT to enable optimal visualization of the in-stent lumen.

CONCLUSION

PCD CT images with HR-plaque kernel enable a more accurate assessment of lumen size and measurements of in-stent plaque portion compared to conventional EID CT images regardless of the stent direction.

Financial support and sponsorship

Nil.

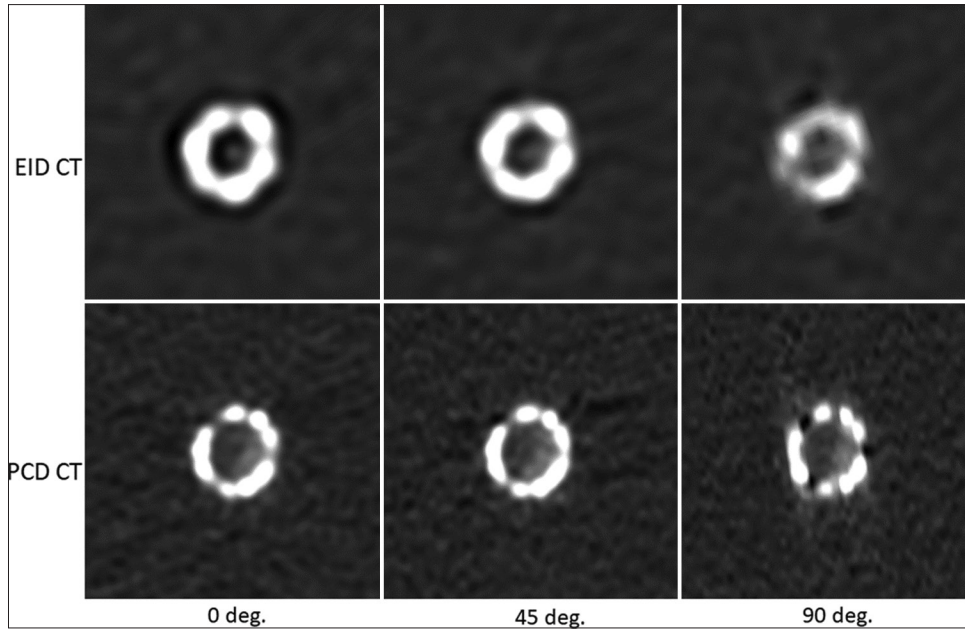


Figure 5: Transverse images at 0°, 45°, and 90° of three stent directions on energy-integrating detector computed tomography (CT) and photon-counting detector CT (PCD CT). PCD CT with high-resolution-plaque kernel improved the visualization of the plaque and iodine-enhanced portions. PCD CT: Photon-counting detector computed tomography, EID CT: Energy-integrating detector CT

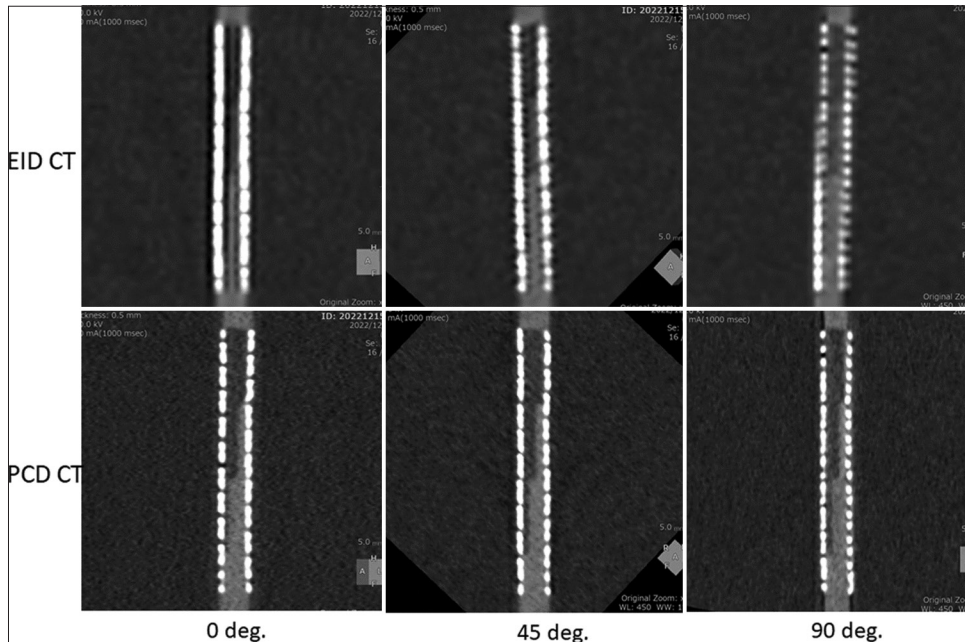


Figure 6: Multiplanar reformation images at 0°, 45°, and 90° of three stent directions on energy-integrating detector computed tomography (EID CT) and photon-counting detector CT (PCD CT). PCD CT with high-resolution-plaque kernel images showed fewer blooming and partial volume artifacts and better separation of plaque and iodine enhancement than EID CT images. PCD CT: Photon-counting detector computed tomography, EID CT: Energy-integrating detector

Conflicts of interest

There are no conflicts of interest.

REFERENCES

1. Mahesh M, Cody DD. Physics of cardiac imaging with multiple-row detector CT. *Radiographics* 2007;27:1495-509.
2. Staniak HL, Bittencourt MS, Pickett C, Cahill M, Kassop D, Slim A, *et al.* Coronary CT angiography for acute chest pain in the emergency department. *J Cardiovasc Comput Tomogr* 2014;8:359-67.
3. Taron J, Lee S, Aluru J, Hoffmann U, Lu MT. A review of serial coronary computed tomography angiography (CTA) to assess plaque progression and therapeutic effect of anti-atherosclerotic drugs. *Int J Cardiovasc Imaging* 2020;36:2305-17.
4. Velusamy R, Nolan M, Murphy A, Thavendiranathan P, Marwick TH. Screening for coronary artery disease in cancer survivors: JACC: Cardiooncology state-of-the-art review. *JACC CardioOncol* 2023;5:22-38.
5. Cassese S, Byrne RA, Schulz S, Hoppman P, Kreutzer J, Feuchtenberger A, *et al.* Prognostic role of restenosis in 10 004 patients

- undergoing routine control angiography after coronary stenting. *Eur Heart J* 2015;36:94-9.
6. Dai T, Wang JR, Hu PF. Diagnostic performance of computed tomography angiography in the detection of coronary artery in-stent restenosis: Evidence from an updated meta-analysis. *Eur Radiol* 2018;28:1373-82.
 7. Narula J, Chandrashekar Y, Ahmadi A, Abbara S, Berman DS, Blankstein R, *et al.* SCCT 2021 expert consensus document on coronary computed tomographic angiography: A report of the society of cardiovascular computed tomography. *J Cardiovasc Comput Tomogr* 2021;15:192-217.
 8. Xu C, Yi Y, Xu M, Yan J, Guo YB, Wang J, *et al.* Coronary artery stent evaluation by CTA: Impact of deep learning reconstruction and subtraction technique. *AJR Am J Roentgenol* 2023;220:63-72.
 9. Mahnken AH, Buecker A, Wildberger JE, Ruebben A, Stanzel S, Vogt F, *et al.* Coronary artery stents in multislice computed tomography: *In vitro* artifact evaluation. *Invest Radiol* 2004;39:27-33.
 10. Mannil M, Hickethier T, von Spiczak J, Baer M, Henning A, Hertel M, *et al.* Photon-counting CT: High-resolution imaging of coronary stents. *Invest Radiol* 2018;53:143-9.
 11. Schroeder S, Achenbach S, Bengel F, Burgstahler C, Cademartiri F, de Feyter P, *et al.* Cardiac computed tomography: Indications, applications, limitations, and training requirements: Report of a writing group deployed by the working group nuclear cardiology and cardiac CT of the European Society of Cardiology and the European Council of Nuclear Cardiology. *Eur Heart J* 2008;29:531-56.
 12. Taylor AJ, Cerqueira M, Hodgson JM, Mark D, Min J, O'Gara P, *et al.* ACCF/SCCT/ACR/AHA/ASE/ASNC/NASCI/SCAI/SCMR 2010 appropriate use criteria for cardiac computed tomography. A report of the American College of Cardiology Foundation Appropriate use criteria task force, the society of cardiovascular computed tomography, the American College of Radiology, the American Heart Association, the American Society of Echocardiography, the American Society of Nuclear Cardiology, the North American Society for Cardiovascular Imaging, the Society for Cardiovascular Angiography and Interventions, and the Society for Cardiovascular Magnetic Resonance. *J Am Coll Cardiol* 2010;56:1864-94.
 13. Flohr T, Petersilka M, Henning A, Ulzheimer S, Ferda J, Schmidt B. Photon-counting CT review. *Phys Med* 2020;79:126-36.
 14. Rajagopal JR, Farhadi F, Richards T, Nikpanah M, Sahbaee P, Shanbhag SM, *et al.* Evaluation of coronary plaques and stents with conventional and photon-counting CT: Benefits of high-resolution photon-counting CT. *Radiol Cardiothorac Imaging* 2021;3:e210102.
 15. Rajendran K, Petersilka M, Henning A, Shanblatt ER, Schmidt B, Flohr TG, *et al.* First clinical photon-counting detector CT system: Technical evaluation. *Radiology* 2022;303:130-8.
 16. Sartoretti T, Wildberger JE, Flohr T, Alkadhi H. Photon-counting detector CT: Early clinical experience review. *Br J Radiol* 2023;96:20220544.
 17. Nakamura Y, Higaki T, Kondo S, Kawashita I, Takahashi I, Awai K. An introduction to photon-counting detector CT (PCD CT) for radiologists. *Jpn J Radiol* 2023;41:266-82.
 18. Cury RC, Leipsic J, Abbara S, Achenbach S, Berman D, Bittencourt M, *et al.* CAD-RADS™ 2.0 – 2022 coronary artery disease-reporting and data system: An expert consensus document of the Society of Cardiovascular Computed Tomography (SCCT), the American College of Cardiology (ACC), the American College of Radiology (ACR), and the North America Society of Cardiovascular Imaging (NASCI). *JACC Cardiovasc Imaging* 2022;15:1974-2001.
 19. Ghekiere O, Salgado R, Buls N, Leiner T, Mancini I, Vanhoenacker P, *et al.* Image quality in coronary CT angiography: Challenges and technical solutions. *Br J Radiol* 2017;90:20160567.
 20. Gebhard C, Fiechter M, Fuchs TA, Stehli J, Müller E, Stähli BE, *et al.* Coronary artery stents: Influence of adaptive statistical iterative reconstruction on image quality using 64-HDCT. *Eur Heart J Cardiovasc Imaging* 2013;14:969-77.
 21. Hou Y, Ma Y, Fan W, Wang Y, Yu M, Vembar M, *et al.* Diagnostic accuracy of low-dose 256-slice multi-detector coronary CT angiography using iterative reconstruction in patients with suspected coronary artery disease. *Eur Radiol* 2014;24:3-11.
 22. Kojima T, Shirasaka T, Yamasaki Y, Kondo M, Hamasaki H, Mikayama R, *et al.* Importance of the heart rate in ultra-high-resolution coronary CT angiography with 0.35 s gantry rotation time. *Jpn J Radiol* 2022;40:781-90.